Supplementary information to Peters *et al.* "Wound-healing defect of CD18$^{-/-}$ mice due to a decrease in TGF-β_1 and myofibroblast differentiation"

Supplementary data 1 (Figure S1). Local injection of TGF-β_1 does not restore PMN recruitment in CD18$^{-/-}$ mice. H&E stainings were prepared from paraffin-embedded sections of CD18$^{-/-}$ and WT mice using wounds 6 h, 24 h, 5 and 7 days after wounding which had been injected with either TGF-β_1 or NaCl. Extravasated PMN within the dermis of the wound margins were identified by morphology and counted in 10 high power fields (HPF) at 40x magnification on a light microscope. Data are given in mean calculated out of 10 HPF. * P <0.05; ** P <0.005.

Supplementary data 2 (Figure S2): Enhanced release of pro-inflammatory cytokines by CD18$^{-/-}$ macrophages *in vitro*. Mature BM-derived macrophages from CD18$^{-/-}$ and WT mice were incubated in presence of 20 ng LPS (purified from E. coli; Sigma)/ml DMEM for 24 h at 37°C and 5% CO_2. Supernatants were harvested and subjected to ELISA for murine IL-1α, IL-1β and IL-6, according to the manufacturer's protocols (all R&D Systems). Data are depicted as the mean ± SD. * P <0.05, ** P <0.005.

Supplementary data 3 (Figure S3). Phagocytosis as such and the associated release of active TGF-β_1 is not impaired in CD18$^{-/-}$ macrophages. To address whether in the absence of CD18, phagocytosis as such is still functional or whether a general incapability of phagocytosis could have caused a defective uptake of apoptotic PMN (**A**) and an impaired secretion of active TGF-β_1 (**B**), CD18$^{-/-}$ (Mϕ^-) or WT (Mϕ^+) macrophages were co-cultured with latex beads (L) (FluoSpheres® 2.0-µm yellow/green-fluorescent microspheres; Molecular Probes, Karlsruhe, Ger-

many) instead of apoptotic PMN, indicative of receptor-independent phagocytosis (Iyoda *et al*, 2002). (**A**) Phagocytosis of latex beads by $CD18^{-/-}$ macrophages was only slightly but not significantly reduced. (**B**) The release of active TGF-β_1, concomitant to latex beads phagocytosis, by $CD18^{-/-}$ macrophages was significantly reduced compared to WT macrophages, although not at all down to levels occurring without latex beads or apoptotic PMN, or in presence of cytochalasin B/C fully blocking the phagocytic machinery. These data demonstrate that the reduced uptake of apoptotic PMN in the absence of CD18 does rather not reflect a general incapability of phagocytosis of $CD18^{-/-}$ macrophages, nor a complete impairment to secrete active TGF-β_1. – To further distinguish base level secretion of active TGF-β_1 from macrophages induced by mere adhesional interaction with apoptotic PMN from specific uptake-induced (phagocytotic) release of active TGF-β_1, experiments were repeated in the presence of the actin-filament polymerisation-blocking agents cytochalasin B and C. The latter substances have been previously reported to selectively block phagocytotic uptake of cells whereas they do not interfere with the secretion of various cytokines (Demuth *et al*, 1996; Painter *et al*, 1981) or CD18 avidity (Katagiri *et al*, 1996). In brief, $CD18^{-/-}$ ($M\phi^-$) or WT ($M\phi^+$) macrophages were pre-incubated for 30 min in complete DMEM containing 2 µg/ml cytochalasin B, or cytochalasin C (both from Sigma), at 37°C in an atmosphere of 5% CO_2. Apoptotic $CD18^{-/-}$ (N^-) or WT (N^+) PMN, or latex beads (L) were added and supernatants for ELISA measurement of active TGF-β_1 were taken 24 h later. Data are depicted as the mean ± SD. * P <0.05, ** P <0.005. (**B**) As biological controls for release of active TGF-β_1 identifying background-level release of TGF-β_1 from dying/necrotic cells during co-culturing, similar experiments were done at 4°C for a period of 24 h, and compared to incubation at 37°C (Figure 6A). Data are given as the mean ± SD.

Supplementary data 4 (Figure S4): Macrophage phenotype in $CD18^{-/-}$ mice. (**A**) BM-derived macrophages isolated from $CD18^{-/-}$ and WT were compared by FACS phenotyping using staining for the macrophage differentiation markers F4/80, MOMA-2, ICAM-1 and scavenger receptor class B (CD36). These markers showed a highly similar expression pattern on $CD18^{-/-}$ and WT BM-derived macrophages, indicating that CD18 deficiency does not affect the *in vitro* maturation and differentiation of murine BM-derived macrophages. (**B**) BM-derived (left graph) and mature peritoneal (right graph) $CD18^{-/-}$ (-) or WT (+) macrophages (Mϕ) were co-cultured with apoptotic $CD18^{-/-}$ or WT PMN in a similar *in vitro* setting as shown in Fig. 6A. After 24 h, supernatants of co-cultures were subjected to ELISA to detect active TGF-β_1. Data are given as the mean ± SD. $^{*,\#}$ P <0.05. (**C**) $CD18^{-/-}$ peritoneal macrophages behave similar to BM-derived macrophages regarding the impaired phagocytosis. Mature peritoneal macrophages were obtained as described in the Supplementary material and methods section, and co-incubated with apoptotic PMN. After 45 min, non-adherent cells were removed by washing. Adherent cells were collected from the well bottoms, stained and analysed by flow cytometry (for details see Supplementary material and methods given below). Phagocytosis was assessed by calculating the percentage of macrophages phagocytosing PMN among total macrophages counted. Bars indicate median of each cohort. ** P <0.005. (**D**) Representative flow-cytometric raw data of the phagocytosis assay presented in (**C**) are provided. Peritoneal macrophages were stained using F4/80 FITC mAb; apoptotic PMN were loaded with CMRA prior to co-culturing for 45 min (for details see Supplementary material and methods given below). Cells appearing in the upper right quadrant of dot plots stain positive for both markers representing macrophages phagocytosing PMN (dot plots given in upper row), as also verified by fluorescence microscopy (data not shown). Besides, a dot plot showing only WT macrophages cultured without apoptotic PMN is provided as control (lower row).

Both release of active TGF-β_1 (supplementary data S4B) and phagocytosis (Figure S4C, D) occurred with similar differences between $CD18^{-/-}$ and WT for peritoneal macrophages as previously found for BM-derived macrophages indicating that both peritoneal and BM-derived macrophages share identical CD18-dependent mechanisms for phagocytosis of apoptotic PMN, mediated via adhesion, and leading to the subsequent release of active TGF-β_1, independent of their origin or stage of maturation.

Supplementary data 5 (Figure S5). Ablation of CD18 function results in a reduced release of IL-8 and its murine homologues, MIP-2 and KC, from macrophages during phagocytosis of apoptotic PMN and analogously, during early phases of wound healing; however, MIP-2 and/or KC do not affect wound contraction in the murine LAD1 model. – Since PMN are almost lacking in wounds of $CD18^{-/-}$ mice, we were interested whether CD18 deficiency, apart from deficient TGF-β_1 release, may also result in a reduced release of other chemokines involved in PMN recruitment. (**A, C**) Therefore, murine MIP-2 and KC concentrations were determined in the supernatants of either $CD18^{-/-}$ or WT macrophages after phagocytosis of apoptotic PMN of the $CD18^{-/-}$ or WT genotype, using an identical procedure for lysates preparation as employed previously for the measurements of TGF-β_1 (see main text, Material and methods section). (**B, D**) In addition, wound lysates at different time points after wounding (2 min, 2 h, 24 h, 5 and 7 days) were subjected to MIP-2- and KC-specific ELISAs according to the manufacturer's protocols (all R&D Systems). (**E**) Human PMN and macrophages were isolated according to the Supplementary material and methods section. PMN were rendered apoptotic and, after incubation with CD18-blocking mAbs at saturating concentration, were subjected to the phagocytosis assay with macrophages, which had either been pre-incubated with CD18-blocking mAbs or had been left untreated. IL-8 was determined from supernatants after 24 h of co-culture using specific ELISA

for human IL-8 (R&D Systems). (**F**) IL-8 homologues were shown to stimulate myofibroblast differentiation in the chicken (Feugate *et al*, 2002) a model system which is considered to reflect IL-8 effects/biology closely to the human situation (Li *et al*, 2005). For ethical reasons, it is not possible to test exogenously injected recombinant human IL-8 for its myofibroblast differentiation-inducing properties and its effect on wound contraction in standardised wounds of LAD1 patients. In order to circumvent this difficulty, we assessed wound contraction in the murine LAD1 model after injection of the murine IL-8 homologues, MIP-2 and KC alone or in combination. To locally supply MIP-2 and/or KC at the wound site, carrier-free recombinant murine MIP-2 or KC (Peprotech, Rocky Hill, NJ) were injected subcutaneously at 3 sites around the wounds, allowing to infiltrate wound margins at a total dose of 1 µg/wound (for doses and procedure see (Khan *et al*, 2004), 2 min after wounding. This time point was selected, as wound lysates revealed significantly lower amounts of MIP-2 and KC in wounds of $CD18^{-/-}$ mice compared to WT, while at 24 h and at any studied later time points (5 and 7 days) no significant reduction in MIP-2 and KC concentration was found in wound lysates of $CD18^{-/-}$ mice. – We did not observe any rescuing effect of MIP-2, KC or MIP-2 and KC regarding the increased wound sizes in $CD18^{-/-}$ mice indicating that the initial decrease in the IL-8 homologues MIP-2 and KC had most likely not been responsible for the delay in wound contraction in $CD18^{-/-}$ mice.

Supplementary data 6 (Figure S6). Bleeding time and platelet numbers are normal in $CD18^{-/-}$ mice. (**A**) Platelet counts were determined from EDTA-treated whole blood samples of $CD18^{-/-}$ or WT mice. (**B**) To assess gross platelet function in $CD18^{-/-}$ and WT mice, subaquatic bleeding times were measured. Mice were immobilised in a device and their tails were kept in 37°C warm water for 2 min. The tails were then incised with a razor blade to induce bleeding from the tail vein and immediately after incising, tails were again put in the water. The time from the start of

bleeding until the bleeding ceased was assessed. Data are depicted as the mean ± SD; n.s., non-significant.

Supplementary data 7 (Figure S7). In co-cultures of macrophages with apoptotic PMN, adhesion is detected at 15 min whereas at 45 min phagocytosis prevails. (**A**) To assess frequency of adhesion and phagocytosis at different time points of co-culturing of macrophages and apoptotic PMN, co-culture assays were performed as described previously (Fig. 6 of main text; supplementary material and methods). Prior to co-culturing, macrophages were stained using F4/80 TriColor (clone Cl:A3-1; Caltag) mAb and apoptotic PMN were loaded with CMRA. After 15 min or 45 min, respectively, non-adherent PMN were removed from plates by washing and the remaining cell conjugates were stained using Ly-6G FITC (clone 1A8; BD Pharmingen) to specifically stain PMN that were still extracellularly adherent and not yet ingested. Samples were then subjected to FACS analysis. Panel **A** shows all $CMRA^{\pm}$ events (i.e. all cell-conjugates that include CMRA-loaded PMN either in an adhesional or in a phagocytotic process) as detected by FACS and subsequently gated upon. Cell-conjugates gated for CMRA positivity were then further analysed for their expression of Ly-6G indicating binding of apoptotic PMN ($Ly\text{-}6G^{\pm}$) to macrophage cell surface (events counted within boxes, given as percentage of total $CMRA^{\pm}$ cell conjugates detected). PMN already ingested by macrophages are only detected as $CMRA^{\pm}$ but do not stain for Ly-6G. This data shows that after 15 min of co-culturing, adhesive processes dominate by far (>90%) between macrophages and apoptotic PMN, independent of the CD18 expression. In contrast, phagocytosis of PMN by macrophages prevails after 45 min of co-culturing. Interestingly, phagocytosis in the WT setting was slightly higher (>95%, with a remaining adhesion below 5%) than in the $CD18^{-/-}$ setting (>85%, with a remaining adhesion below 15%), although this difference was not quite significant when all analysed samples (n=3) were

subjected to statistics (P>0.05). Representative dot plots are given. (**B**) PMN adherence to and phagocytosis by macrophages was assessed in immunofluorescence microscopy. For this, apoptotic PMN (loaded with LysoSensor Green, a pH-dependent fluorescent dye) were incubated with macrophages for 15 min to assess adhesion and 45 min to investigate phagocytosis. After co-culture, non-adherent cells were washed and microscopic pictures were recorded digitally overlaying differential interference contrast (DIC, using Nomarsky optics) with fluorescence pictures. Phagocytosis did almost not occur in WT or $CD18^{-/-}$ co-cultures at 15 min, as shown by the absence or very low intensity level of fluorescence at this time point (upper panel, left: FITC, and right: merge DIC and FITC; representative pictures for both $CD18^{-/-}$ and WT co-cultures), indicating that LysoSensor Green specifically distinguishes between adhesion (no fluorescence) and phagocytosis (pH-dependent increase in fluorescence). At 45 min the dominating event was phagocytosis, as pointed out by the increase in the fluorescence intensity of the LysoSensor loaded in PMN entering the acidified medium of the activated macrophage. Also an impaired capacity of the $CD18^{-/-}$ macrophages to engulf $CD18^{-/-}$ apoptotic PMN could be observed (middle panel, left: FITC, and right: merge DIC and FITC) when compared with the WT co-culture (lower panel, left: FITC and right: merge DIC and FITC). The bar represents 40 µm.

Supplementary material and methods

Isolation of peritoneal macrophages

Peritoneal macrophages served as a source of *in vivo*-generated mature macrophages (Rutherford *et al*, 1993), and were obtained according to established procedures (Cohn and Benson, 1965). Briefly, the peritoneal cavities of $CD18^{-/-}$ and WT mice (n=4) were lavaged with 5 ml ice-cold calcium/magnesium-free PBS. Peritoneal cells were collected by centrifugation of the lavage fluid and resuspended at a concentration of $2x10^6$/ ml DMEM supplemented with 10% heat-inactivated FCS, 2% L-Glutamine, 1% penicillin/streptomycin and 1% non-essential aminoacids. The cell suspension was plated onto 24 well dishes at $2x10^6$/ ml/well and left to adhere for 2 h at 37°C in a humidified 5% CO_2 atmosphere. Non-adherent cells were removed by washing 3 times with PBS. Adherent cells were then incubated over night in fresh DMEM/FCS and used for co-culture experiments the next day.

Adhesion and phagocytosis assays

For fluorescence microscopy, 6 days old mature WT and $CD18^{-/-}$ mouse macrophages were plated out on poly-D-lysine-coated slides at 10^6cells/ml DMEM and left to adhere for 24h at 37°C in a humidified 5% CO_2 atmosphere. PMNs isolated as described above from WT and $CD18^{-/-}$ mice were stained with the intracellular dye CMRA (red/orange fluorescing) (Molecular Probes) at 5 µM final concentration. Staining was done at 37°C and 5% CO_2 for 30 min, followed by washing. PMNs were then rendered apoptotic by ageing as described and co-cultured with macrophages for 15 min and 45 min to assess adhesion and phagocytosis, respectively. After co-culture, non-adherent PMN were washed, slides were covered with fluorescent mounting medium (Dako) and the proportion of macrophages ingesting PMN was counted, in an analogous fashion as previously described (Fadok *et al*, 1998; Fadok *et al*, 2001), only this time using immuno-

fluorescence microscopy with a Zeiss Axioscop 2 microscope equipped with appropriate fluorescence filters. Microscopic pictures were recorded digitally overlaying differential interference contrast (DIC, using Nomarsky optics) with fluorescence pictures as supported by AxioVision® software (Carl Zeiss Inc.).

In another set of experiments PMN were loaded with the fluorescent pH indicator LysoSensor Green (DND-189; Molecular Probes) at 1 µM final concentration. Staining was done at 37°C and 5% CO_2 for 30 min, followed by washing. This dye, not fluorescent under neutral pH conditions, accumulates in acidic organelles, especially lysosomes, as a result of protonation and exhibits a pH-dependent increase in fluorescence intensity upon acidification. PMN were then and co-cultured with macrophages for 15 min and 45 min to assess adhesion and phagocytosis, respectively. In this system we could distinguish between the process of adhesion – where the dye does not reach the lysosomal machinery of the macrophages and thus is not induced to fluoresce – and phagocytosis, where labelled PMN enter the phagocyte and, in the acidified milieu of the activated macrophage, fluorescence is induced.

For additional large-scale quantification, co-cultures were also subjected to FACS analyses after the indicated interaction times. Macrophages and PMN were adjusted separately to a concentration $1x10^8$ cells/ml. CMRA (orange-fluorescing; Molecular Probes) was added to the PMN suspension in order to obtain 1 µM final concentration. Staining was done at 37°C and 5% CO_2 for 30 min, followed by one washing and subsequent co-culture as depicted above. In a second setting, PMN were not stained before co-cultures. In this case, cell conjugates were stained immediately after co-cultures using Ly-6G FITC (clone 1A8; BD Pharmingen) at 1 µg/ml to specifically stain PMN that still were extracellularly adherent and not yet ingested. After the indicated interaction periods, cell conjugates were additionally double-stained with F4/80 TriColor (clone Cl:A3-1; Caltag) to dye macrophages and with annexin-V APC to detect extra-

cellularly adherent PMN. Samples were then measured with a CellQuest Pro®-supported FACS-Calibur.

Isolation of human monocytes and PMN

Human monocytes and PMN were isolated as described elsewhere (Ezekowitz *et al*, 1985). Briefly, fresh whole blood from healthy volunteers was centrifuged on Ficoll-Paque (Amersham, Freiburg, Germany). Mononuclear cells were resuspended in RPMI 1640 supplemented with 2% L-Glutamine and Penicillin/Streptomycin 100 U/µg/ml at $2x10^6$/ml, left to adhere for 1 h in 24-well tissue culture plates (Nunc) and then washed to remove non-adherent cells. Cells were further cultivated at 37°C and 5% CO_2 for 5 days. After 5 days the adherent cells were assessed for the mature macrophage marker 25F9 (Zwadlo *et al,* 1985) by flow cytometry. Seventy to 80% of the cells were positive for 25F9 (data not shown). Mononuclear cells from two LAD1 patients were a kind gift from Dr. Wilhelm Friedrich, Dept. of Pediatrics, University of Ulm). Rest expression of CD18 on these cells, as assessed by flow cytometry using PE-coupled anti-CD18 mAb (clone 6.7; BD Pharmingen) was less than 0.5% in both patients thus representing severe type LAD1.

PMN were obtained by adding the pellet from the Ficoll-Paque gradient to 3% dextran (Amersham) and further lysis with ammonium chloride buffer of the remaining erythrocytes. Apoptosis of PMN was induced by aging for 20 h of $5x10^6$/ml PBS at 37°C and was assessed by flow cytometry by using annexin-V FITC (BD Pharmingen). For adhesion and phagocytosis assays, PMN were stained with the intracellular dye CMRA (Molecular Probes).

Adhesion and phagocytosis assay with human monocytes/macrophages and PMN

Two different anti-CD18 mAb – clone IB4 as an $F(ab)_2$ fragment to avoid F_c receptor binding (Ancell, Bayport, MN) (Wright *et al*, 1983) and clone TS1/18 (BioLegend, San Diego, CA) (Diacovo *et al*, 1996) – were used in separate serum-free co-culture experiments to block CD18 either on macrophages, PMN or both. PMN were incubated with saturating concentrations of IB4 (10 µg/ml), respectively TS1/18 (20 µg/ml) for 15 min (both achieving identically high blocking of CD18 receptor in these respective concentrations), washed and co-cultured in different experimental settings. For adhesion assay, macrophages were incubated with PMN for 15 min at 37°C, 5% CO_2 and humidified atmosphere, detached by scrapping, stained for 25F9 and analysed by flow cytometry. For phagocytosis assay, the incubation time was 45 min. Cytokine release was measured after 24 h of co-culture under the same conditions.

Characterisation of BM-derived macrophages from WT and CD18$^{-/-}$ mice

Six-day-old BM-derived macrophages from WT and CD18$^{-/-}$ mice were stained for the macrophage-specific marker F4/80 (clone Cl:A3-1, conjugated with Alexa Fluor 488; Caltag Laboratories GmbH, Germany), for the macrophage/monocyte marker 2 (clone MOMA-2 FITC; Serotec, Düsseldorf, Germany), for the LFA-1 and MAC-1 ligand ICAM-1 (CD54 PE, clone 3E2; Caltag) and for the scavenger receptor B (CD36 FITC, clone CRF D-2712; BD Pharmingen) and the expression of these markers was then analysed with a CellQuest Pro®-supported FACSCalibur.

References to supplementary data

Cohn ZA, Benson B (1965) The in vitro differentiation of mononuclear phagocytes. 3. The reversibility of granule and hydrolytic enzyme formation and the turnover of granule constituents. *J Exp Med* **122:** 455-466

Demuth A, Goebel W, Beuscher HU, Kuhn M (1996) Differential regulation of cytokine and cytokine receptor mRNA expression upon infection of bone marrow-derived macrophages with Listeria monocytogenes. *Infect Immun* **64:** 3475-3483

Diacovo TG, Roth SJ, Buccola JM, Bainton DF, Springer TA (1996) Neutrophil rolling, arrest, and transmigration across activated, surface-adherent platelets via sequential action of P-selectin and the beta 2-integrin CD11b/CD18. *Blood* **88:** 146-157

Ezekowitz RA, Sim RB, MacPherson GG, Gordon S (1985) Interaction of human monocytes, macrophages, and polymorphonuclear leukocytes with zymosan in vitro. Role of type 3 complement receptors and macrophage-derived complement. *J Clin Invest* **76:** 2368-2376

Fadok VA, Bratton DL, Konowal A, Freed PW, Westcott JY, Henson PM (1998) Macrophages that have ingested apoptotic cells in vitro inhibit proinflammatory cytokine production through autocrine/paracrine mechanisms involving TGF-beta, PGE2, and PAF. *J Clin Invest* **101:** 890-898

Fadok VA, de Cathelineau A, Daleke DL, Henson PM, Bratton DL (2001) Loss of phospholipid asymmetry and surface exposure of phosphatidylserine is required for phagocytosis of apoptotic cells by macrophages and fibroblasts. *J Biol Chem* **276:** 1071-1077

Feugate JE, Li Q, Wong L, Martins-Green M (2002) The cxc chemokine cCAF stimulates differentiation of fibroblasts into myofibroblasts and accelerates wound closure. *J Cell Biol* **156:** 161-172

Iyoda T, Shimoyama S, Liu K, Omatsu Y, Akiyama Y, Maeda Y, Takahara K, Steinman RM, Inaba K (2002) The CD8+ dendritic cell subset selectively endocytoses dying cells in culture and in vivo. *J Exp Med* **195:** 1289-1302

Katagiri K, Kinashi T, Irie S, Katagiri T (1996) Differential regulation of leukocyte function-associated antigen-1/ intercellular adhesion molecules-1-dependent adhesion and aggregation in HL-60 cells. *Blood* **87:** 4276-4285

Khan AI, Kerfoot SM, Heit B, Liu L, Andonegui G, Ruffell B, Johnson P, Kubes P (2004) Role of CD44 and hyaluronan in neutrophil recruitment. *J Immunol* **173:** 7594-7601

Li QJ, Yao M, Dueck M, Feugate JE, Parpura V, Martins-Green M (2005) cCXCR1 is a receptor for cIL-8 (9E3/cCAF) and its N- and C-terminal peptides and is also activated by hIL-8 (CXCL8). *J Leukoc Biol* **77:** 421-431

Painter RG, Whisenand J, McIntosh AT (1981) Effects of cytochalasin B on actin and myosin association with particle binding sites in mouse macrophages: implications with regard to the mechanism of action of the cytochalasins. *J Cell Biol* **91:** 373-384

Rutherford MS, Witsell A, Schook LB (1993) Mechanisms generating functionally heterogeneous macrophages: chaos revisited. *J Leukoc Biol* **53:** 602-618

Wright SD, Rao PE, Van Voorhis WC, Craigmyle LS, Iida K, Talle MA, Westberg EF, Goldstein G, Silverstein SC (1983) Identification of the C3bi receptor of human monocytes and macrophages by using monoclonal antibodies. *Proc Natl Acad Sci U S A* **80:** 5699-5703

Zwadlo G, Brocker EB, von Bassewitz DB, Feige U, Sorg C (1985) A monoclonal antibody to a differentiation antigen present on mature human macrophages and absent from monocytes. *J Immunol* **134:** 1487-1492

Fig. S1

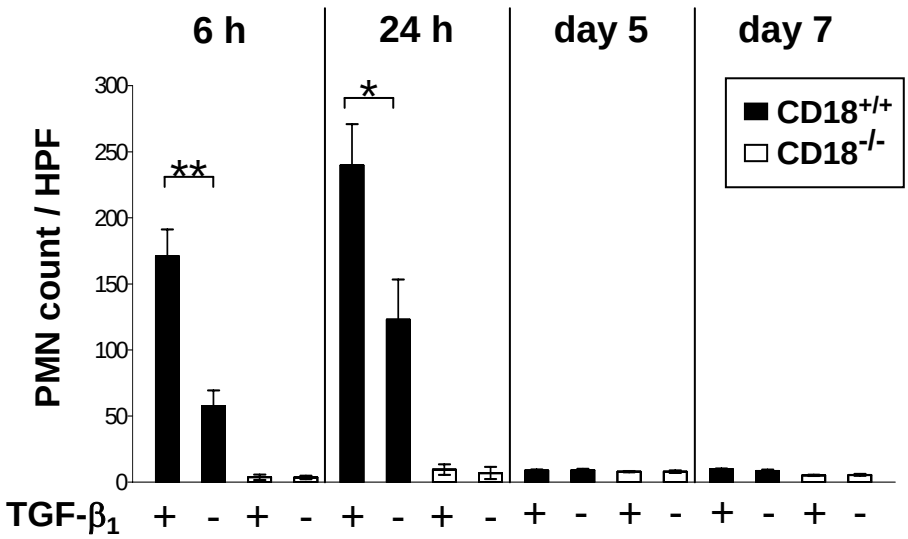
6 h
24 h
day 5
day 7
PMN count / HPF
300
250
200
150
100
50
0
**
*
CD18+/+
CD18-/-
TGF-β1
+ - + - + - + - + - + - + - + -

Fig. S2

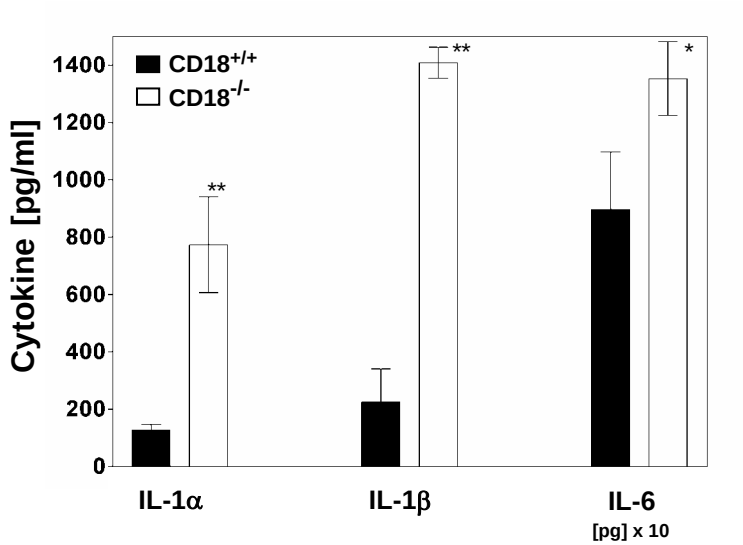
CD18+/+
CD18-/-
Cytokine [pg/ml]
1400
1200
1000
800
600
400
200
0
**
**
*
IL-1α
IL-1β
IL-6
[pg] x 10

Fig. S3

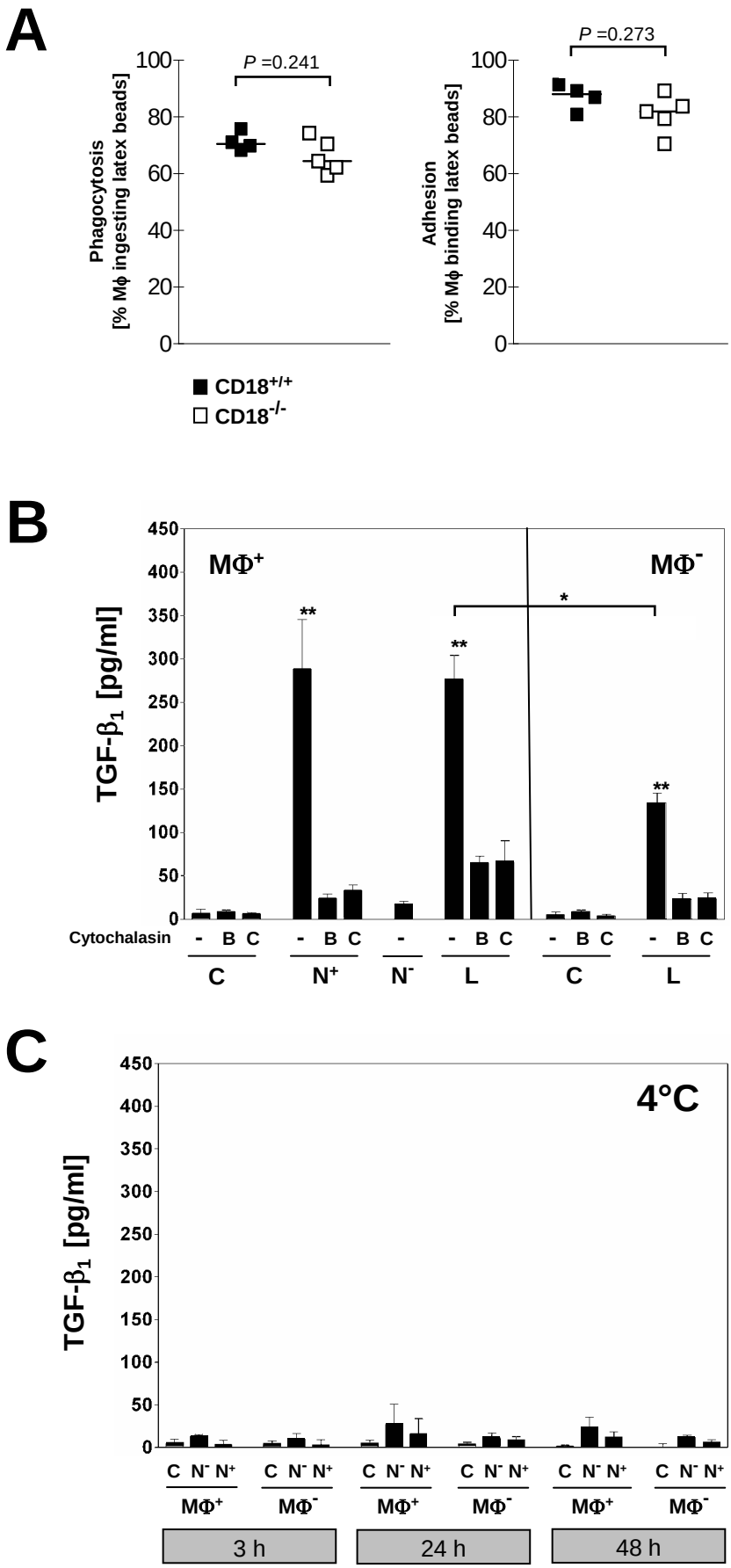
A
P =0.241
P =0.273
Phagocytosis [% Mϕ ingesting latex beads]
Adhesion [% Mϕ binding latex beads]
100
80
60
40
20
0
CD18+/+
CD18-/-
B
MΦ+
MΦ-
TGF-β1 [pg/ml]
450
400
350
300
250
200
150
100
50
0
**
*
Cytochalasin
- B C
C
N+
N-
L
C
L
C
4°C
TGF-β1 [pg/ml]
C N- N+
MΦ+
MΦ-
3 h
24 h
48 h

Fig. S4

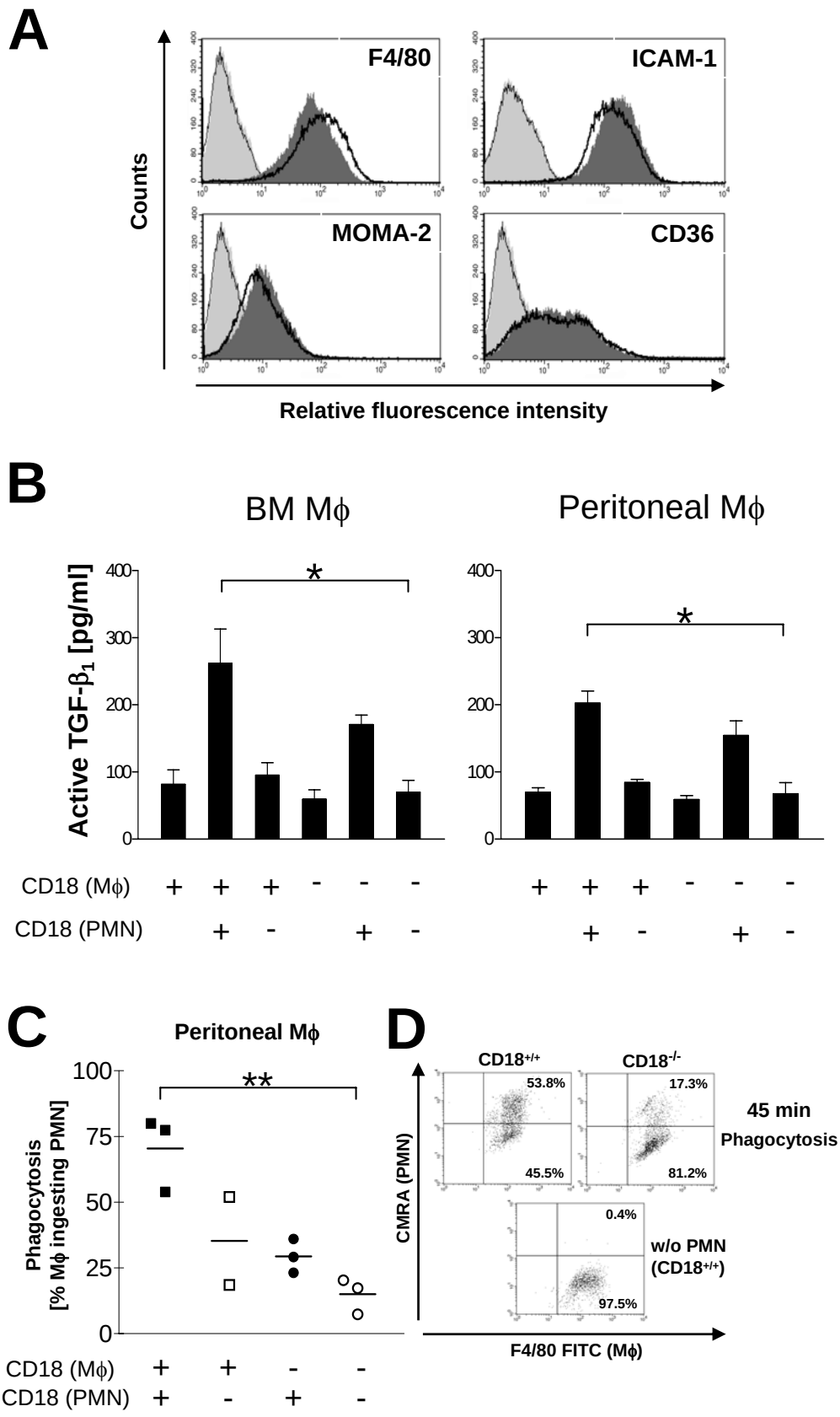
A
F4/80
ICAM-1
MOMA-2
CD36
Counts
Relative fluorescence intensity
B
BM Mϕ
Peritoneal Mϕ
Active TGF-β1 [pg/ml]
400
300
200
100
0
*
*
CD18 (Mϕ) + + + - - -
CD18 (PMN) + - + -
C
Peritoneal Mϕ
Phagocytosis [% Mϕ ingesting PMN]
100
75
50
25
0
**
CD18 (Mϕ) + + - -
CD18 (PMN) + - + -
D
CD18+/+
CD18-/-
53.8%
45.5%
17.3%
81.2%
45 min Phagocytosis
0.4%
97.5%
w/o PMN (CD18+/+)
CMRA (PMN)
F4/80 FITC (Mϕ)

Fig. S5

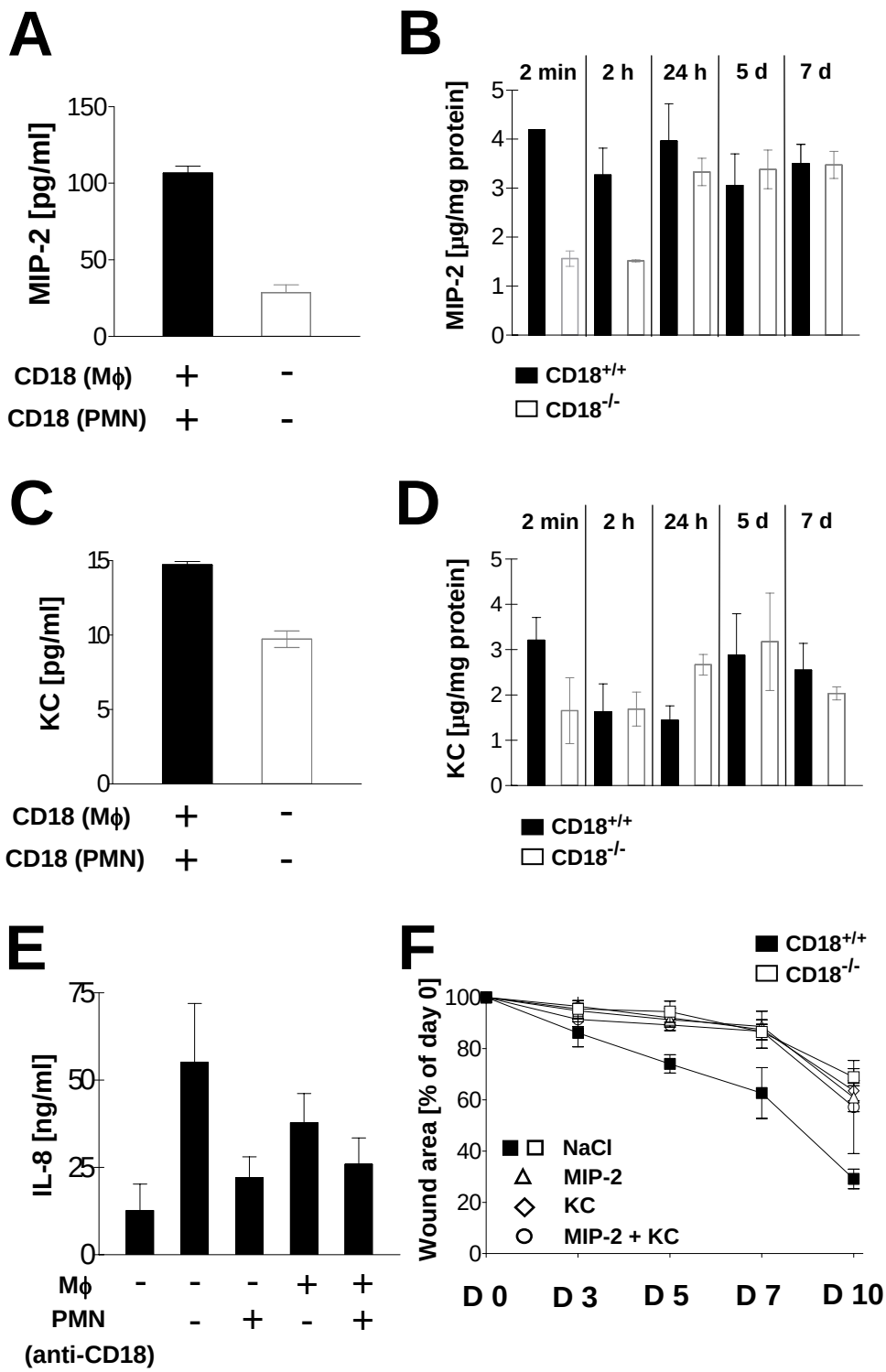
A
MIP-2 [pg/ml]
150
100
50
0
CD18 (Mϕ) + -
CD18 (PMN) + -
B
2 min
2 h
24 h
5 d
7 d
MIP-2 [µg/mg protein]
5
4
3
2
1
0
CD18+/+
CD18-/-
C
KC [pg/ml]
15
10
5
0
CD18 (Mϕ) + -
CD18 (PMN) + -
D
2 min
2 h
24 h
5 d
7 d
KC [µg/mg protein]
5
4
3
2
1
0
CD18+/+
CD18-/-
E
IL-8 [ng/ml]
75
50
25
0
Mϕ - - - + +
PMN - + - +
(anti-CD18)
F
CD18+/+
CD18-/-
Wound area [% of day 0]
100
80
60
40
20
0
NaCl
MIP-2
KC
MIP-2 + KC
D 0
D 3
D 5
D 7
D 10

Fig. S6

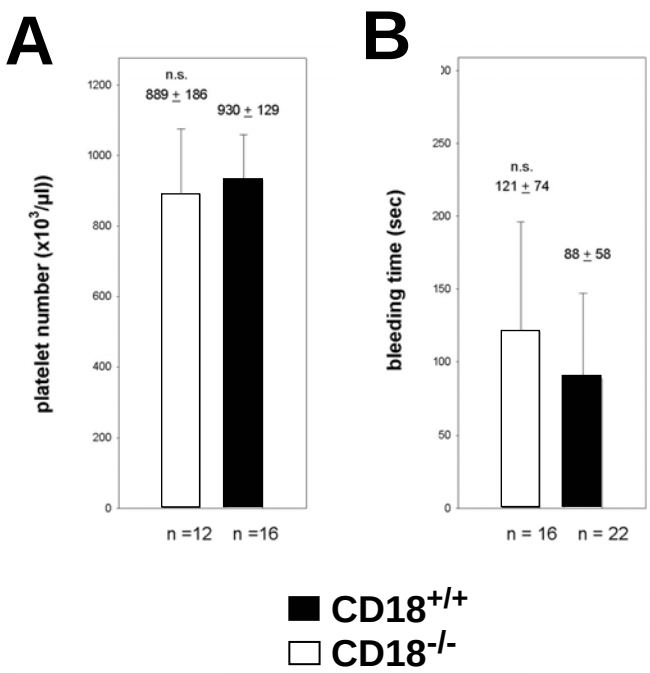
A
B
n.s.
889 ± 186
930 ± 129
platelet number (x10³/µl))
1200
1000
800
600
400
200
0
n =12
n =16
n.s.
121 ± 74
88 ± 58
bleeding time (sec)
250
200
150
100
50
0
n = 16
n = 22
CD18+/+
CD18-/-

Fig. S7

A

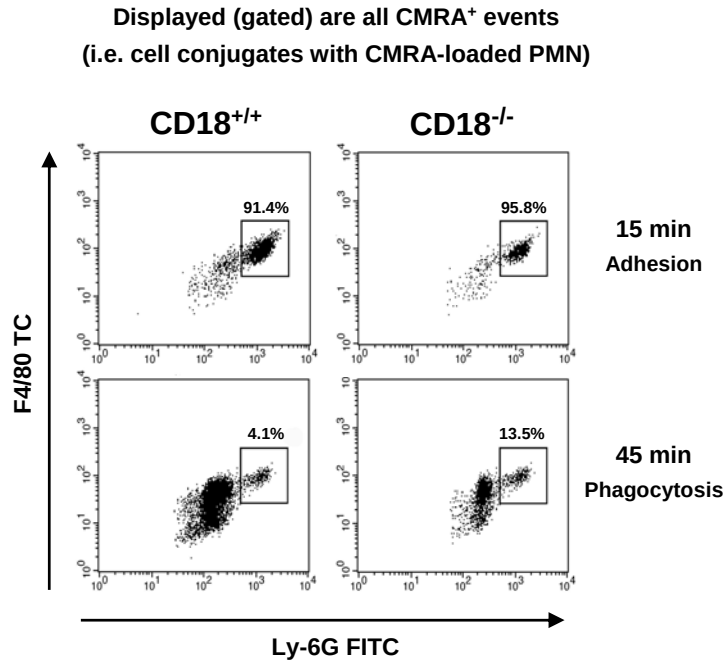
Displayed (gated) are all CMRA+ events
(i.e. cell conjugates with CMRA-loaded PMN)
CD18+/+
CD18-/-
91.4%
95.8%
4.1%
13.5%
15 min
Adhesion
45 min
Phagocytosis
F4/80 TC
Ly-6G FITC

B

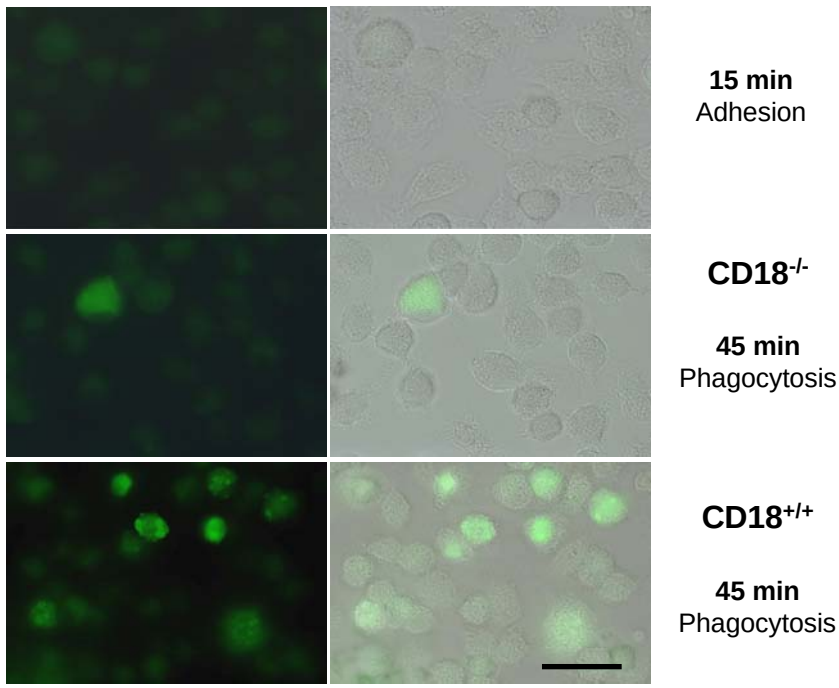
15 min
Adhesion
CD18-/-
45 min
Phagocytosis
CD18+/+
45 min
Phagocytosis